FEBS Letters 587 (2013) 305–310

FEBS Letters
journal homepage: www.FEBSLetters.org

Quaternary structure of human, *Drosophila melanogaster* and *Caenorhabditis elegans* MFE-2 in solution from synchrotron small-angle X-ray scattering

Maija L. Mehtälä [a,1], Tatu J.K. Haataja [a,1,2], Clément E. Blanchet [b,1], J. Kalervo Hiltunen [a], Dmitri I. Svergun [b,*], Tuomo Glumoff [a,*]

[a] Department of Biochemistry and Biocenter Oulu, University of Oulu, P.O. Box 3000, FI-90014 Oulu, Finland
[b] European Molecular Biology Laboratory, Hamburg Outstation c/o DESY, Notkestraße 85, D-22603 Hamburg, Germany

ARTICLE INFO

Article history:
Received 11 September 2012
Revised 22 November 2012
Accepted 14 December 2012
Available online 8 January 2013

Edited by Christian Griesinger

Keywords:
Peroxisome
β-Oxidation
Multifunctional enzyme type 2
Sterol carrier protein 2-like
Synchrotron

ABSTRACT

Multifunctional enzyme type 2 (MFE-2) forms part of the fatty acid β-oxidation pathway in peroxisomes. MFE-2s from various species reveal proteins with structurally homologous functional domains assembled in different compilations. Crystal structures of all domain types are known. SAXS data from human, fruit fly and *Caenorhabditis elegans* MFE-2s and their constituent domains were collected, and both ab initio and rigid body models constructed. Location of the putative substrate binding helper domain SCP-2L (sterol carrier protein 2-like), which is not part of MFE-2 protein in every species and not seen as part of any previous MFE-2 structures, was determined. The obtained models of human and *C. elegans* MFE-2 lend a direct structural support to the idea of the biological role of SCP-2L.

Structured summary of protein interactions:
HsMFE-2 and **HsMFE-2** bind by x ray scattering (View interaction)
CeMFE-2 and **CeMFE-2** bind by x ray scattering (View interaction)
DmMFE-2 and **DmMFE-2** bind by x ray scattering (View interaction)

1. Introduction

Multifunctional enzyme type 2 (MFE-2) is a ubiquitous eukaryotic peroxisomal fatty acid metabolizing protein carrying, in the same polypeptide, two out of four enzymatic activities of the β-oxidation spiral [1,2]. In humans both activities of MFE-2, the 3R-hydroxyacyl-CoA dehydrogenase ("dehydrogenase, DH") and the 2E-enoyl-CoA hydratase 2 ("hydratase 2, H2"), are indispensable, since a metabolic accumulation disease (D-bifunctional protein (D-BP) deficiency) follows from diminished function of either activities [3]. In addition to the enzymatic domains vertebrate and zebrafish MFE-2s have an additional domain, which is homologous and structurally very similar to the unspecific lipid-binding protein sterol carrier protein 2 (SCP-2), and therefore usually referred to as SCP-2L (-like) domain [4,5]. Crystal or NMR structures of all these domains as stand-alone proteins have been solved and structure–function relationships concerning e.g. dimerization, substrate specificity and genotype–phenotype correlation in the D-BP deficiency have been studied [6–13].

Genetic and protein studies have revealed that MFE-2 proteins from different species have been compiled from the above functional domains in different ways (Fig. 1). In the MFE-2 sequence the dehydrogenase domain is always N-terminal, followed by the hydratase 2 and the SCP-2L domains with notable exceptions: (i) *Drosophila melanogaster* and most yeasts represent species devoid of SCP-2L domain, (ii) yeasts have a duplicated dehydrogenase domain preceding the hydratase 2 [14], and (iii) *Caenorhabditis elegans* dehydrogenase forms a fusion protein with the SCP-2L domain while expressing the hydratase 2 as a separate

Abbreviations: MFE-2, peroxisomal multifunctional enzyme type 2; DH, 3R-hydroxyacyl-CoA dehydrogenase; H2, 2E-enoyl-CoA hydratase 2; SCP-2L, sterol carrier protein 2-like; *Dm*, *Drosophila melanogaster*; *Hs*, *Homo sapiens*; *Ce*, *Caenorhabditis elegans*; SAXS, small-angle X-ray scattering; PDB, protein data bank; CoA, coenzyme A; aa, amino acid

* Corresponding authors. Fax: +49 40 89902 149 (D.I. Svergun), fax: +358 8 553 1141 (T. Glumoff).
E-mail addresses: svergun@embl-hamburg.de (D.I. Svergun), tuomo.glumoff@oulu.fi (T. Glumoff).

[1] These authors contributed equally to this work.
[2] Present address: Department of Experimental Medical Science, Lund University, SE-221 84 Lund, Sweden.

0014-5793/$36.00
http://dx.doi.org/10.1016/j.febslet.2012.12.014

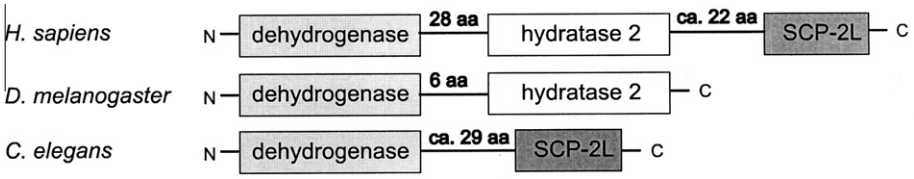

Fig. 1. Domain composition of MFE-2 proteins from human, *D. melanogaster* and *C. elegans*. The domain names dehydrogenase, hydratase 2 and SCP-2L stand for 3R-hydroxyacyl-CoA dehydrogenase, 2E-enoyl-CoA hydratase 2 and sterol carrier protein 2-like, respectively. For clarity, N- and C-termini, connecting loop regions as well as the domains are not in scale. As discussed in the text, the connecting loop between the dehydrogenase and the hydratase 2 domains in the human MFE-2 is considerably longer than in the *Drosophila* protein. The loops separating the SCP-2L domain from the nearest enzymatic domain are of comparable length in the human and the *C. elegans* proteins. aa = amino acid.

polypeptide. While the mutual arrangement of the enzymatic domains in various MFE-2s is known from the crystal structure of the *D. melanogaster* protein (*Dm*MFE-2) [15] it is not known how the SCP-2L domain complements the structural assembly of SCP-2L-containing MFE-2s.

Why do some MFE-2s possess the SCP-2L domain and some others not? Various studies have shown that SCP-2 or SCP-2L domain binds lipids that are known to be substrates for MFE-2, such as long-chain [16] and very long-chain [17] saturated and unsaturated [18] fatty acyl-CoAs and C27-intermediates of bile acid synthesis [19], but they also bind lipids that are not, or not known to be, substrates of MFE-2: free fatty acids [20], phytanoyl-CoA [21], 16-doxylstearic acid [6] and Triton X-100 [8]. The suggested function of SCP-2/SCP-2L is mostly a trafficking/uptake protein carrying lipids between membranes and other lipid-containing cellular objects or a substrate-binding helper domain. Concerning D-BP deficiency in humans, there are no known mutations in the SCP-2L domain that would be responsible for the disease, indicating that either such cases go undetected or that e.g. a point mutation is not enough to impede substrate binding to a generous hydrophobic binding pocket of SCP-2L. On the other hand mice lacking SCP-2 display disrupted cholesterol and biliary lipid metabolism [22] and branched-chain fatty acyl-CoA catabolism [21] indicative of SCP-2 deficiency.

It is unlikely that the function of SCP-2L would not be connected to the function of one or both of the enzymatic activities of MFE-2 and the question remains whether the lipid binding property of SCP-2L contributes to function of the enzymatic domain(s). To enable this functionality, the SCP-2L domain would need to be positioned favorably with respect to the enzyme domain(s). In the present work we employed SAXS to elucidate the solution structures of human (*Hs*MFE-2), *C. elegans* (*Ce*MFE-2) and *Drosophila* (*Dm*MFE-2) proteins. Their domain organization was determined both by ab initio analysis and by hybrid modeling utilizing the crystallographic structures of the individual MFE-2 and *Dm*MFE-2 domains.

2. Materials and methods

2.1. Production and preparation of the samples for SAXS measurements

The recombinant full-length *Dm*MFE-2 and the separate *Dm*DH and *Dm*H2 fragments were expressed in *Eschericia coli* and purified for the SAXS data collection as previously described [15]. The expression and purification of the 2E-enoyl-CoA hydratase 2 fragment of *Hs*MFE-2 also followed the previously described protocol [11]. The human SCP-2L was purified following the same protocol as for *Dm*H2, and the *C. elegans* MFE-2 was purified like the full-length *Dm*MFE-2 [15]. Further details of expression and purification of the proteins for SAXS measurements is given in the Supplementary material.

2.2. SAXS data collection and processing of the data

2.2.1. Data collection

Synchrotron X-ray scattering data were all collected at the EMBL X33 beamline (DESY, Hamburg) [23]. The scattering patterns of all samples were measured at several solute concentrations ranging from 2 to 10 mg/ml. At a sample-detector distance of 2.7 m, the range of momentum transfer $0.1 < s < 5\ \mathrm{nm}^{-1}$ was collected. Primary data processing and evaluation of the overall structural parameters were performed using standard procedure by the program package PRIMUS [24]. The molecular masses of the solutes were evaluated by scaling against the reference solution of bovine serum albumin.

2.2.2. D. melanogaster MFE-2

The dummy bead model of *Dm*MFE-2 is an average of 10 ab initio models built from the SAXS data using the program DAMMIF [25]. Alignment and averaging of the 10 models were done using the programs SUPCOMB [26] and DAMAVER [27].

2.2.3. Human MFE-2

The bead model of *Hs*MFE-2 was constructed by MONSA [28], which simultaneously fits the experimental data of *Dm*MFE-2 and *Hs*MFE-2 to build the two-phase model. The rigid body model was built using the program BUNCH [29] with the crystal structures of *Dm*MFE-2 and the SCP-2L domain of the *Hs*MFE-2 (*Hs*SCP-2L). *Dm*MFE-2 and *Hs*SCP-2L were connected to each other using dummy residues for the missing linkers. A simulated annealing protocol was used to find an interconnected configuration with no steric clashes that produces the best fit to the experimental data.

2.2.4. C. elegans MFE-2

Experimental data of the dehydrogenase domain of *Ce*MFE-2 (*Ce*DH) and *Ce*MFE-2 were simultaneously fitted by the program MONSA [28] to build the multiphase bead model. The program BUNCH [29] uses *Ce*DH and *Hs*SCP2-L domains to fit *Ce*MFE-2 experimental data and build the rigid body model.

3. Results

3.1. D. melanogaster MFE-2

The crystal structure of *Dm*MFE-2 is known at 2.15 Å resolution [15]. It forms a compact 'double dimeric' structure in which both the dehydrogenase and the hydratase 2 from different MFE-2 monomers form dimers (Fig. 2). SAXS structure of *Dm*MFE-2 and its fit with the crystal structure would indicate the value of using *Dm*MFE-2 as a framework for the human protein, which in addition contains the SCP-2L domain in each MFE-2 monomer. SAXS data were collected from the full-length *Dm*MFE-2, the dehydrogenase domain (*Dm*DH), the hydratase 2 domain (*Dm*H2) and the two

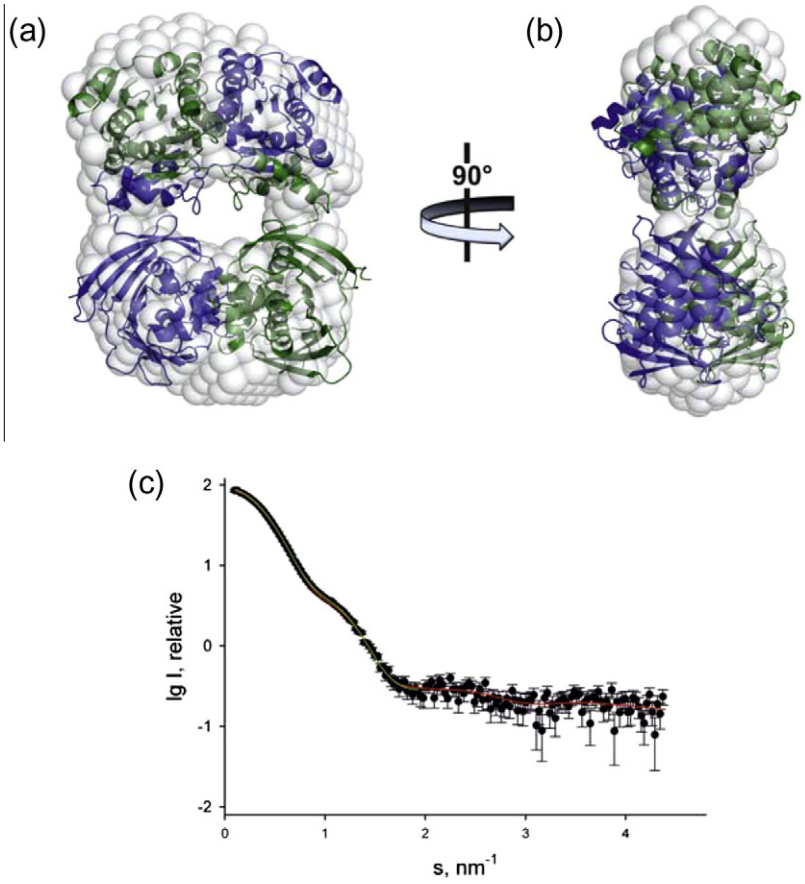

Fig. 2. Ab initio model of *D. melanogaster* MFE-2 (*Dm*MFE-2). (a) SAXS model of *Dm*MFE-2 superimposed with its crystal structure. The ab initio model is presented in white, crystal structures of dehydrogenase–hydratase monomer A in green and monomer B in blue. Dehydrogenase dimer is sited up, hydratase two dimer down. (b) As (a) but turned 90°. (c) Experimental data (dot with error bars) with the fit of the ab initio model scattering pattern (in green) and the theoretical scattering pattern (in red) calculated from the crystallographic structure using the program CRYSOL [30]. The SAXS patterns are displayed as the logarithm of the scattering intensity versus the momentum transfer $s = 4\pi \sin\theta/\lambda$, where λ is the X-ray wavelength (1.5 Å) and 2θ is the scattering angle. For clarity, only one of every 10 experimental points are represented in the figure.

catalytic domains together in the same solution. The calculations done by CRYSOL [30] indicate that a *Dm*MFE-2 monomer alone does not fit the scattering data (results not shown). This is consistent with *Dm*MFE-2 being a dimer like other MFE-2s and standalone MFE-2 domains. If combined for the SAXS data collection *Dm*DH and *Dm*H2 do not spontaneously assemble in vitro to form *Dm*MFE-2, in agreement with results from static light scattering measurements [15].

The ab initio shape of *Dm*MFE-2 representing the enzyme at low resolution in solution highly resembles the overall shape from the high resolution crystal structure of *Dm*MFE-2. When superimposing the ab initio model of *Dm*MFE-2 with the crystal structure the obtained fit of the two models is very good and the volume of the particle in solution is almost completely filled (Fig. 2).

3.2. Human MFE-2

The crystal structure of the SCP-2L domain of *Hs*MFE-2 is known (PDB ID 1IKT), and it is known that the sequence and structural similarities between the individual domains of MFE-2 from various species is high. Assuming a similar structure of the catalytic domains in *Dm* and *Hs*, and using the scattering curves of the full length *Dm* and *HsMFE-2,* two models of *Hs*MFE-2 were obtained using alternative approaches. In one of them, a two-phase ab initio model represents the structure as beads by fitting the experimental scattering curves of *Dm* and *Hs*MFE-2. Here, one phase corresponds to the catalytic domains of MFE-2, which contribute to both scattering curves. The second phase consists of the SCP-2L, only present in the human variant. In the other approach, a rigid body model is constructed corresponding to the configuration of the *Dm* catalytic domains and human SCP-2L domains that fit best the scattering pattern of *Hs*MFE-2. The linkers missing in the PDB files are modeled as dummy residues. As seen from the superposition in Fig. 3, the two models obtained by different methods are consistent with each other.

The total volume, radius of gyration and D_{max} are larger in the human MFE-2 in comparison with the corresponding values from *Dm*MFE-2 (see Supplementary data). This was to be expected since the *Dm* variant lacks the SCP-2L domain. The actual location of the SCP-2L domains on the opposite sides of the dimer is consistent with the fact that also the active sites of the hydratase 2 domains are situated respectively [11]. Since the crystal structure of *Hs*MFE-2 is presently unknown, no direct comparison of the experimental scattering with the theoretical scattering of the full-length protein can be made.

3.3. C. elegans MFE-2

Crystal structures of the full length *Ce*MFE-2 or its individual domains are not available. The sequence homology between the dehydrogenase and SCP-2L domains of *Ce*MFE-2 compared with the corresponding domains of human MFE-2 is high, allowing us to use the same approach for SAXS structure determination as used for *Dm*MFE-2 and *Hs*MFE-2. Several datasets of the *C. elegans* MFE-

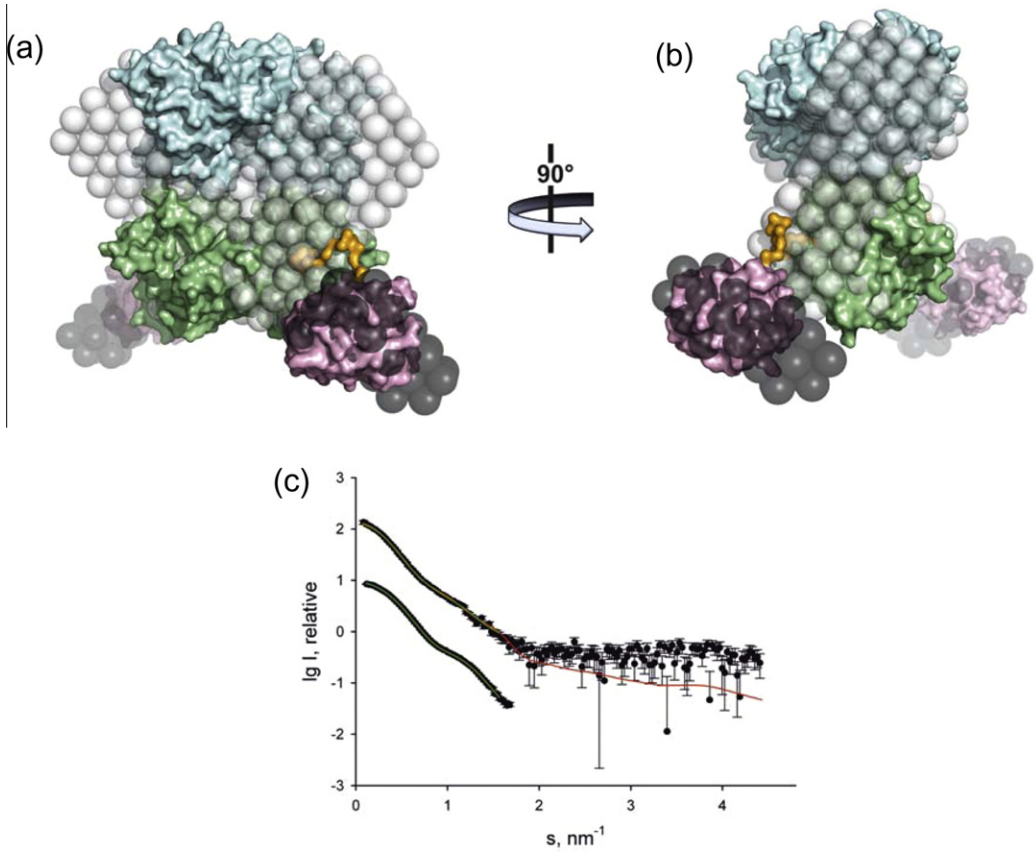

Fig. 3. Ab initio and rigid body models of human MFE-2 (*Hs*MFE-2). (a) A two-phase ab initio model superimposed with the rigid body model of the full length *Hs*MFE-2. The ab initio model depicts the catalytic domains (light grey beads) and the SCP-2L domains (dark grey beads). The dehydrogenase is displayed in pale cyan, hydratase 2 in pale green, SCP-2L in light pink and linkers in orange. (b) As (a) but turned 90°. (c) Experimental data of *Hs*MFE-2 and *Dm*MFE-2 with the fit of the ab initio (green) and rigid body (red) models. For clarity, the curves are offset along the logarithmic axis and only one of every 10 experimental points is represented.

2 were collected, as well as data from the separate hydratase 2 enzyme (*Ce*H2) and the two polypeptides together in the same solution (*Ce*MFE-2 + *Ce*H2). The two-phase ab initio model was built using the experimental curves of *Ce*DH and of the full length *Ce*MFE2, with one phase consisting of the DH domains and the other phase the SCP-2L domains. In addition, a rigid body model was constructed using the human dehydrogenase and SCP-2L structures as building blocks by fitting the *Ce*MFE-2 scattering data (Fig. 4). The linkers connecting the domains are missing in the PDB files, and they are modeled as dummy residues. The consistency between the superimposed ab initio and rigid body models is high, and both models fit well the experimental data of *Ce*MFE-2. Measuring the *Ce*MFE-2 and the *Ce*H2 together showed clearly that these proteins do not self-assemble.

4. Discussion

Volumes and shapes of the SAXS models from different species presented in this study provide structural envelopes with striking similarity between the species where available constituent domain crystal structures could be fit well. This indicates high quality of the protein samples and of the SAXS data as well as high similarity between the static crystal structures and the potentially dynamic low resolution solution shapes. Firstly, as expected, the shape of the double dimeric core part of *Hs*MFE-2 (dehydrogenase and hydratase 2 domains) is similar to that of *Dm*MFE-2. It is thus likely that the formation of the dimer of the two catalytic dimers in *Dm*MFE-2 and *Hs*MFE-2 is very similar despite much longer connecting linkers between the enzymatic domains in the latter (Fig. 1). Since the distances between the active sites remain similar in both of these MFE-2s it is more probable that the longer linkers in *Hs*MFE-2 are extending outside of the compact core structure rather than folding inside. Secondly, assembly of the SCP-2L domain of the two SCP-2L-containing MFE-2s (human and *C. elegans*) resemble each other with the domain positioned in the vicinity of the substrate binding pocket of the immediate enzyme domain in spite of the fact that the enzyme which they are connected to is different (Fig. 1). The crystal structures of *Hs*DH and *Hs*SCP-2L fit well in the volume provided by ab initio model of *Ce*MFE-2. Despite the revealed assembly of the full-length proteins the structural details do not allow to draw precise conclusions regarding the direction to which the hydrophobic pockets of the SCP-2L domains are facing.

In the SAXS models the locations of the enzyme dimers could easily be determined, yet the low resolution does not allow to unambiguously differentiating between the dehydrogenase dimer and the hydratase 2 dimer. However, the locations of the SCP-2L domains in the *Hs*MFE-2 structure offer a solution to this problem.

The data also clearly indicate that if *Dm*MFE-2, and *Ce*MFE-2 are supplemented in the SAXS data collection with the "missing domain" (i.e. SCP-2L in the case of *Dm*MFE-2 and *Ce*H2 in the case of *Ce*MFE-2) they do not assemble into heterodimers to produce an assembly resembling human MFE-2.

Based on the present models one could speculate about possible conformational changes upon cofactor (NAD^+ for dehydrogenase) and 3R-hydroxyacyl-CoA substrate binding. The *Dm*MFE-2 and the corresponding core part of *Hs*MFE-2 are rather compact and considerable amount of protein surface is engaged in dimerization. *Dm*MFE-2 and *Hs*MFE-2 are in this respect very similar despite the

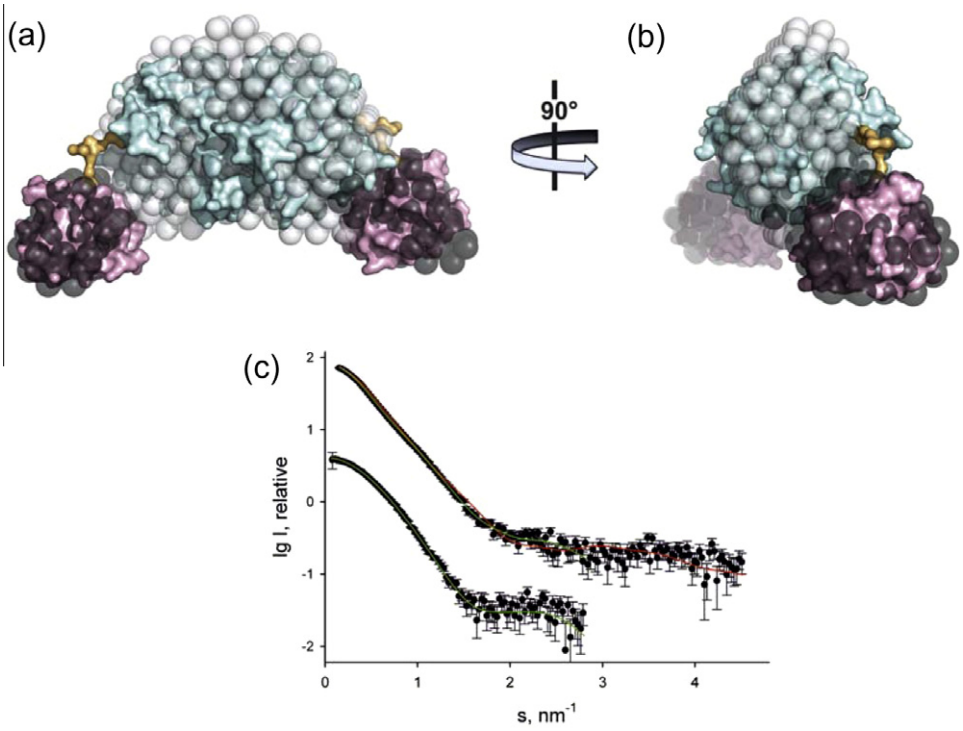

Fig. 4. Ab initio and rigid body models of *C. elegans* (*Ce*MFE-2). (a) The two-phase ab initio model superimposed with the rigid body model of *Ce*MFE-2. The color coding is as in Fig. 3(a). (b) As (a) but turned 90°. (c) Experimental data (dot with error bars) of *Ce*DH and *Ce*MFE2 with the fits of the ab initio (green) and rigid body (red) models. For clarity, the curves are offset along the logarithmic axis and only one of every 10 experimental points is represented.

aforementioned linker length difference. It could therefore be argued that the structures are rather static and large movements of the catalytic domains are not likely (possibly limited to subtle rearrangements of the secondary structures or loops at entry cavities).

The linker lengths separating the hydratase 2 domain and the SCP-2L in *Hs*MFE-2 and the dehydrogenase and SCP-2L domains in *Ce*MFE-2 are both long, above 20 amino acids (Fig. 1). This allows us to speculate on the role of the small lipid binding domain in the catalytic reaction(s) of *Hs*MFE-2. In theory, the length of the linker may allow the SCP-2L domain to shuttle between the catalytic domains. In this sense the role of SCP-2L domain could simply be auxiliary by fishing bulky and poorly water soluble substrates from the aqueous bulk and subsequently feeding them to the hydratase 2 subunit of MFE-2. After the hydration, the intermediate could, instead of temporarily diffusing into the surrounding solvent, be fetched again by SCP-2L and further presented to the dehydrogenase active site. In the case of *Ce*MFE-2 the SCP-2L domain could be a receptor receiving the substrate from the separate hydratase 2 protein. The hydrophobic pocket provided by the SCP-2L domain is very suitable for temporary accommodation of the MFE-2 substrates and the flexibility provided by the connecting loop support the idea of a role for SCP-2L in the enzymatic reactions. It remains to be determined experimentally whether this is the case, however.

Despite sufficient amounts of pure proteins for crystallization screenings and extensive utilization of different methods, no crystals of *Hs*MFE-2 or other SCP-2L-containing MFE-2s (*Ce*MFE-2 and HSDL2 (human hydroxysteroid dehydrogenase-like 2) [31]) have been obtained (T.J.K.H. & M.L.M., unpublished results). On the contrary, crystallizing *Dm*MFE-2 and several SCP-2s as stand-alone proteins was straightforward. This may indicate that in the context of the full length MFE-2 polypeptide the SCP-2L domain is mobile and counter-effects crystallization. Our SAXS study did provide low resolution structural model of SCP-2L-containing MFE-2s. The obtained locations of the SCP-2L domains most likely represent an average over the conformational space explored by the domain and it may prove to be challenging to obtain high resolution data about the maximum boundaries between which the SCP-2L domain is able to move.

Acknowledgments

This work was supported by the Academy of Finland (Grant number 1122531 (to T. Glumoff)); and the Sigrid Jusélius Foundation and the Academy of Finland (Grant number 138690 (to K. Hiltunen)). Data were collected at the EMBL SAXS beamline X33 at the DORIS storage ring, DESY, Hamburg, Germany. We thank Dr. Kristian Koski and Ville Ratas for excellent technical assistance, and Prof. Lloyd Ruddock for providing us with the pLWRP51 plasmid. D.I. Svergun acknowledges the support by the EU infrastructures grants WeNMR (contract number: 261572) and BioStruct-X (contract number: 283570).

Appendix A. Supplementary data

Supplementary data associated with this article can be found, in the online version, at http://dx.doi.org/10.1016/j.febslet.2012.12.014.

References

[1] Hiltunen, J.K., Wenzel, B., Beyer, A., Erdmann, R., Fossa, A. and Kunau, W.H. (1992) Peroxisomal multifunctional beta-oxidation protein of *Saccharomyces cerevisiae*. Molecular analysis of the fox2 gene and gene product. J. Biol. Chem. 267, 6646–6653.

[2] Adamski, J., Normand, T., Leenders, F., Monte, D., Begue, A., Stehelin, D., Jungblut, P.W. and de Launoit, Y. (1995) Molecular cloning of a novel widely expressed human 80 kDa 17 beta-hydroxysteroid dehydrogenase IV. Biochem. J. 311 (Pt 2), 437–443.

[3] van Grunsven, E.G., van Berkel, E., Ijlst, L., Vreken, P., de Klerk, J.B., Adamski, J., Lemonde, H., Clayton, P.T., Cuebas, D.A. and Wanders, R.J. (1998) Peroxisomal D-hydroxyacyl-CoA dehydrogenase deficiency: resolution of the enzyme defect and its molecular basis in bifunctional protein deficiency. Proc. Natl. Acad. Sci. USA 95, 2128–2133.
[4] Noland, B.J., Arebalo, R.E., Hansbury, E. and Scallen, T.J. (1980) Purification and properties of sterol carrier protein2. J. Biol. Chem. 255, 4282–4289.
[5] Edqvist, J. and Blomqvist, K. (2006) Fusion and fission, the evolution of sterol carrier protein-2. J. Mol. Evol. 62, 292–306.
[6] Garcia, F.L., Szyperski, T., Dyer, J.H., Choinowski, T., Seedorf, U., Hauser, H. and Wuthrich, K. (2000) NMR structure of the sterol carrier protein-2: implications for the biological role. J. Mol. Biol. 295, 595–603.
[7] Choinowski, T., Hauser, H. and Piontek, K. (2000) Structure of sterol carrier protein 2 at 1.8 Å resolution reveals a hydrophobic tunnel suitable for lipid binding. Biochemistry 39, 1897–1902.
[8] Haapalainen, A.M., van Aalten, D.M., Merilainen, G., Jalonen, J.E., Pirila, P., Wierenga, R.K., Hiltunen, J.K. and Glumoff, T. (2001) Crystal structure of the liganded SCP-2-like domain of human peroxisomal multifunctional enzyme type 2 at 1.75 Å resolution. J. Mol. Biol. 313, 1127–1138.
[9] Haapalainen, A.M., Koski, M.K., Qin, Y.M., Hiltunen, J.K. and Glumoff, T. (2003) Binary structure of the two-domain (3R)-hydroxyacyl-CoA dehydrogenase from rat peroxisomal multifunctional enzyme type 2 at 2.38 Å resolution. Structure 11, 87–97.
[10] Koski, M.K., Haapalainen, A.M., Hiltunen, J.K. and Glumoff, T. (2004) A two-domain structure of one subunit explains unique features of eukaryotic hydratase 2. J. Biol. Chem. 279, 24666–24672.
[11] Koski, K.M., Haapalainen, A.M., Hiltunen, J.K. and Glumoff, T. (2005) Crystal structure of 2-enoyl-CoA hydratase 2 from human peroxisomal multifunctional enzyme type 2. J. Mol. Biol. 345, 1157–1169.
[12] Ferdinandusse, S., Denis, S., Mooyer, P.A., Dekker, C., Duran, M., Soorani-Lunsing, R.J., Boltshauser, E., Macaya, A., Gartner, J., Majoie, C.B., Barth, P.G., Wanders, R.J. and Poll-The, B.T. (2006) Clinical and biochemical spectrum of D-bifunctional protein deficiency. Ann. Neurol. 59, 92–104.
[13] Ylianttila, M.S., Pursiainen, N.V., Haapalainen, A.M., Juffer, A.H., Poirier, Y., Hiltunen, J.K. and Glumoff, T. (2006) Crystal structure of yeast peroxisomal multifunctional enzyme: structural basis for substrate specificity of (3R)-hydroxyacyl-CoA dehydrogenase units. J. Mol. Biol. 358, 1286–1295.
[14] Breitling, R., Marijanovic, Z., Perovic, D. and Adamski, J. (2001) Evolution of 17beta-HSD type 4, a multifunctional protein of beta-oxidation. Mol. Cell. Endocrinol. 171, 205–210.
[15] Haataja, T.J., Koski, M.K., Hiltunen, J.K. and Glumoff, T. (2011) Peroxisomal multifunctional enzyme type 2 from the fruitfly: dehydrogenase and hydratase act as separate entities, as revealed by structure and kinetics. Biochem. J. 435, 771–781.
[16] Frolov, A., Cho, T.H., Billheimer, J.T. and Schroeder, F. (1996) Sterol carrier protein-2, a new fatty acyl coenzyme A-binding protein. J. Biol. Chem. 271, 31878–31884.
[17] Dansen, T.B., Westerman, J., Wouters, F.S., Wanders, R.J., van Hoek, A., Gadella Jr, T.W. and Wirtz, K.W. (1999) High-affinity binding of very-long-chain fatty acyl-CoA esters to the peroxisomal non-specific lipid-transfer protein (sterol carrier protein-2). Biochem. J. 339 (Pt 1), 193–199.
[18] Ferreyra, R.G., Burgardt, N.I., Milikowski, D., Melen, G., Kornblihtt, A.R., Dell'Angelica, E.C., Santome, J.A. and Ermacora, M.R. (2006) A yeast sterol carrier protein with fatty-acid and fatty-acyl-CoA binding activity. Arch. Biochem. Biophys. 453, 197–206.
[19] Colles, S.M., Woodford, J.K., Moncecchi, D., Myers-Payne, S.C., McLean, L.R., Billheimer, J.T. and Schroeder, F. (1995) Cholesterol interaction with recombinant human sterol carrier protein-2. Lipids 30, 795–803.
[20] Stolowich, N.J., Frolov, A., Atshaves, B., Murphy, E.J., Jolly, C.A., Billheimer, J.T., Scott, A.I. and Schroeder, F. (1997) The sterol carrier protein-2 fatty acid binding site: an NMR, circular dichroic, and fluorescence spectroscopic determination. Biochemistry 36, 1719–1729.
[21] Seedorf, U., Raabe, M., Ellinghaus, P., Kannenberg, F., Fobker, M., Engel, T., Denis, S., Wouters, F., Wirtz, K.W., Wanders, R.J., Maeda, N. and Assmann, G. (1998) Defective peroxisomal catabolism of branched fatty acyl coenzyme A in mice lacking the sterol carrier protein-2/sterol carrier protein-x gene function. Genes Dev. 12, 1189–1201.
[22] Fuchs, M., Hafer, A., Munch, C., Kannenberg, F., Teichmann, S., Scheibner, J., Stange, E.F. and Seedorf, U. (2001) Disruption of the sterol carrier protein 2 gene in mice impairs biliary lipid and hepatic cholesterol metabolism. J. Biol. Chem. 276, 48058–48065.
[23] Blanchet, C.E., Zozulya, A.V., Kikhney, A.G., Franke, D., Konarev, P.V., Shang, W., Klaering, R., Robrahn, B., Hermes, C., Cipriani, F., Svergun, D.I. and Roessle, M. (2012) Instrumental setup for high-throughput small- and wide-angle solution scattering at the X33 beamline of EMBL Hamburg. J. Appl. Crystallogr. 45, 489–495.
[24] Konarev, P.V., Volkov, V.V., Sokolova, A.V., Koch, M.H.J. and Svergun, D.I. (2003) *PRIMUS*: a Windows PC-based system for small-angle scattering data analysis. J. Appl. Crystallogr. 36, 1277–1282.
[25] Franke, D. and Svergun, D.I. (2009) *DAMMIF*, a program for rapid *ab initio* shape determination in small-angle scattering. J. Appl. Crystallogr. 42, 342–346.
[26] Kozin, M.B. and Svergun, D.I. (2001) Automated matching of high- and low-resolution structural models. J. Appl. Crystallogr. 34, 33–41.
[27] Volkov, V.V. and Svergun, D.I. (2003) Uniqueness of *ab initio* shape determination in small-angle scattering. J. Appl. Crystallogr. 36, 860–864.
[28] Svergun, D.I. (1999) Restoring low resolution structure of biological macromolecules from solution scattering using simulated annealing. Biophys. J. 76, 2879–2886.
[29] Petoukhov, M.V. and Svergun, D.I. (2005) Global rigid body modeling of macromolecular complexes against small-angle scattering data. Biophys. J. 89, 1237–1250.
[30] Svergun, D., Barberato, C. and Koch, M.H.J. (1995) CRYSOL – a program to evaluate X-ray solution scattering of biological macromolecules from atomic coordinates. J. Appl. Crystallogr. 28, 768–773.
[31] Dai, J., Xie, Y., Wu, Q., Wang, L., Yin, G., Ye, X., Zeng, L., Xu, J., Ji, C., Gu, S., Huang, Q., Zhao, R.C. and Mao, Y. (2003) Molecular cloning and characterization of a novel human hydroxysteroid dehydrogenase-like 2 (HSDL2) cDNA from fetal brain. Biochem. Genet. 41, 165–174.